AIP Applied Physics Letters

Molybdenum oxide MoOx: A versatile hole contact for silicon solar cells

James Bullock, Andres Cuevas, Thomas Allen, and Corsin Battaglia

Citation: Applied Physics Letters **105**, 232109 (2014); doi: 10.1063/1.4903467
View online: http://dx.doi.org/10.1063/1.4903467
View Table of Contents: http://scitation.aip.org/content/aip/journal/apl/105/23?ver=pdfcov
Published by the AIP Publishing

Molybdenum oxide MoO_x: A versatile hole contact for silicon solar cells

James Bullock,[1,a)] Andres Cuevas,[1] Thomas Allen,[1] and Corsin Battaglia[2]
[1]*Research School of Engineering, The Australian National University, Canberra ACT 0200, Australia*
[2]*Empa, Swiss Federal Laboratories for Materials Science and Technology, 8600 Dübendorf, Switzerland*

(Received 22 October 2014; accepted 11 November 2014; published online 9 December 2014)

This letter examines the application of transparent MoO_x ($x < 3$) films deposited by thermal evaporation directly onto crystalline silicon (*c*-Si) to create hole-conducting contacts for silicon solar cells. The carrier-selectivity of MoO_x based contacts on both n- and p-type surfaces is evaluated via simultaneous consideration of the contact recombination parameter J_{0c} and the contact resistivity ρ_c. Contacts made to p-type wafers and p^+ diffused regions achieve optimum ρ_c values of 1 and 0.2 mΩ·cm^2, respectively, and both result in a J_{0c} of ~200 fA/cm^2. These values suggest that significant gains can be made over conventional hole contacts to p-type material. Similar MoO_x contacts made to n-type silicon result in higher J_{0c} and ρ_c with optimum values of ~300 fA/cm^2 and 30 mΩ·cm^2 but still offer significant advantages over conventional approaches in terms of contact passivation, optical properties, and device fabrication.
[http://dx.doi.org/10.1063/1.4903467]

The spatial separation of light-generated electron-hole pairs is critical to the functionality of all photovoltaic devices. The segregation of electrons and holes towards their respective contact regions requires the formation of pathways of asymmetric electron and hole conductivity.[1] The majority of crystalline silicon (*c*-Si) solar cells achieve this by introducing a high concentration of dopants (usually phosphorus, aluminium, or boron) in the near-surface regions of the *c*-Si wafer. The dopant species increase the concentration of (and hence, conductivity for) one charge carrier, whilst having the opposite effect for the other. This approach is particularly advantageous for directly metalized silicon contacts as the metal-silicon interface suffers from both large majority carrier resistance and high minority carrier recombination, both of which can be reduced by heavy surface doping. However, the high majority carrier concentration within the doped regions also causes significant Auger recombination, introducing a fundamental limit on the possible reduction of recombination. The lowest recombination parameters for heavily doped, metal-contacted regions have experimentally been found to be ~300 fA/cm^2 for phosphorus,[2] ~400 fA/cm^2 for boron,[3] and higher still for aluminium alloyed[4] regions (J_0 values have been adjusted in accordance with the intrinsic carrier concentration used in this letter $n_i = 8.6 \times 10^9\,\text{cm}^{-3}$). This limitation has prompted the development of device designs with small contact fractions where the total minority carrier recombination can be reduced at the expense of increased majority carrier resistance—a trade-off which is usually permissible given their relative impact on solar cell performance. However, difficulties associated with the transferral of small contact fractions to industrial pilot lines have led to research into alternative means of separating carriers and contacting solar cells.

An alternative strategy to achieve carrier-selectivity is via the application of thin layers of materials on the *c*-Si absorber that provide an asymmetry in carrier conductivity. Cell architectures utilising such materials have recently demonstrated world record efficiencies on *c*-Si,[5,6] outperforming their dopant diffused counterparts. Not surprisingly, research into suitable electron and hole collecting layers on *c*-Si is currently a popular topic, with some groups transferring layers commonly used for the same purpose from non-*c*-Si based solar cells. For example, organic polymer,[7,8] transition metal oxide,[9–12] and transparent conductive oxide[13,14] based contacts, which are standard in other photovoltaic technologies, have recently been demonstrated on *c*-Si. Among these contacting schemes, the use of sub-stoichiometric molybdenum oxide MoO_x ($x < 3$) stands out as particularly attractive given its ease of deposition and already demonstrated performance on *c*-Si.[9,10] This letter examines the application of MoO_x directly to *c*-Si to create a hole-transporting contact for *c*-Si solar cells.

Molybdenum trioxide MoO_3 is a wide band-gap material (~3 eV) with an exceptionally large electron affinity (~6.7 eV) and ionisation energy (~9.7 eV).[10,15] When deposited by vacuum evaporation from a solid MoO_3 source, as is the case in this letter, a slightly sub-stoichiometric (MoO_x, $_{x<3}$) amorphous film results.[9,16] The reduced Mo oxidation state results in the formation of a defect band below the conduction band and provides the film with a semi-metallic, n-type character.[10,15,16] The conductivity of MoO_x films has been shown to vary by more than ten orders of magnitude in transitioning from the insulating MoO_3, with reported conductivities as low as 10^{-7} S/cm, to the semi-metallic MoO_2 which exhibits conductivities in the range of 10^4 S/cm.[15,17] Gains in conductivity are typically weighed against transparency and work function—both of which are found to decrease with a decreasing oxidation state.[15,18]

The most significant characteristic of thermally evaporated MoO_x films is their large chemical potential of up to ~6.9 eV—much higher than that of the elemental metals, a characteristic that they share with two other sub-stoichiometric transition metal oxides: VO_x and WO_x. Amongst these three oxides, MoO_x has the additional advantage of a low melting point, which assists in maintaining a high oxidation state and a low thermal budget when evaporating.

a)james.bullock@anu.edu.au

When MoO_x is applied to *c*-Si, the large chemical potential difference between the two materials induces a balancing electrostatic potential which falls partially across both materials and, if Fermi-level pinning is present, across the interface. Whilst Fermi-level pinning is pervasive at elemental metal/*c*-Si interfaces, it is still unknown to what extent it affects the MoO_x/*c*-Si interface, and it has recently been suggested that MoO_x can partially alleviate this effect for transition-metal dichalcogenides.[17] In the event of weak or no Fermi-level pinning at the MoO_x/*c*-Si interface, a hole accumulation layer on p-type *c*-Si and a hole inversion layer on n-type *c*-Si would be expected—facilitating low resistance hole transport out of the *c*-Si absorber.

In this letter, the application of MoO_x to *c*-Si is investigated to form simple hole contacts in three different configurations. These are categorised as "accumulation" type contacts to (i) lightly doped p-type silicon (referred to hereafter ***pSi***/MoO_x contact), (ii) heavily boron doped silicon (referred to hereafter as $\boldsymbol{p^+Si}$/MoO_x contact), and (iii) an "inversion" type contact to low resistivity n-type silicon (referred to hereafter as ***nSi***/MoO_x contact).

The efficacy of the ***pSi***/MoO_x, $\boldsymbol{p^+Si}$/MoO_x, and ***nSi***/MoO_x hole contacts, that is, their selectivity towards holes, is assessed via their recombination and resistive properties. The contact recombination parameter J_{0c} (as determined from carrier lifetime test structures) provides information on the undesired "conductivity" presented to electrons towards the *c*-Si/MoO_x interface, whilst the contact resistivity ρ_c (as determined from contact resistance test structures) indicates the detrimental resistance to holes. Improved hole-selectivity is achieved via simultaneous minimisation of J_{0c} and ρ_c.

All test structures were fabricated on (100) oriented, float-zone, *c*-Si substrates. The wafer resistivities of the ***pSi***/MoO_x and ***nSi***/MoO_x structures were ~2.1 Ω·cm and ~4.2 Ω·cm, respectively, whilst the $\boldsymbol{p^+Si}$/MoO_x contact structures were fabricated on 100 Ω·cm n-type wafers with front and rear surface boron diffusions (surface concentration $N_{surf} \sim 1 \times 10^{19}\,cm^{-3}$ and sheet resistance $R_{sh} \sim 110$ Ω/□). Test structures were RCA cleaned and immersed in a 1% HF solution immediately prior to MoO_x deposition. MoO_x films of 3–80 nm thickness were thermally evaporated at a rate of ~1 Å/s from a MoO_3 powder source (99.95% purity) with a base pressure of $<7 \times 10^{-7}$ Torr.

Lifetime test structures were prepared by depositing MoO_x on both wafer surfaces. A thin palladium (Pd) (<10 nm) over-layer was evaporated onto the MoO_x to mimic a device contact, whilst still allowing sufficient light transmission for the injection dependent carrier lifetime to be measured by the photoconductance decay technique. The J_{0c} values were extracted from the measured effective carrier lifetimes using the Kane and Swanson technique[19] with an n_i value of $8.6 \times 10^{-9}\,cm^{-3}$ (at 25 °C). This technique, originally applied to characterise dopant diffused wafer surfaces (like the $\boldsymbol{p^+Si}$/MoO_x contact), has been shown to also be valid for undiffused wafers with strongly inverted or accumulated surfaces,[20] as is expected for the ***pSi***/MoO_x and ***nSi***/MoO_x contacts.

Contact resistance test structures were made by depositing MoO_x on one side of a *c*-Si sample, following which a Pd (40 nm)/Al (1 μm) metal stack was evaporated on top through a shadow mask to create the desired contact structure pattern. For the ***nSi***/MoO_x and $\boldsymbol{p^+Si}$/MoO_x contact structures, a transfer-length-method (TLM) contact pad array was used to measure ρ_c. Whilst the use of the TLM procedure on heavily diffused surfaces is well accepted,[21] its application to low resistivity wafers with a surface inversion layer has only been explored briefly.[22,23] In this approach, we have assumed that current flows are confined to the inversion layer. The sheet resistance of this inversion layer is also measurable by the TLM.

For the ***pSi***/MoO_x contacts, ρ_c was measured using the method devised by Cox and Strack.[24] For this measurement, an Ohmic rear contact, formed by evaporated aluminium, was assumed to contribute negligibly to the total measured resistance, rendering the extracted ρ_c an upper limit for the ***pSi***/MoO_x ρ_c. All current voltage (I-V) measurements were taken in the dark using a Keithley 2425 source-meter at ~23 °C. The ρ_c values presented here are without a sintering step. It should be noted that in all contact structures used in this study, the extracted ρ_c comprises the resistance of the MoO_x/*c*-Si and MoO_x/Pd interfaces as well as the MoO_x bulk resistivity. In addition, whilst Pd was used in this instance, less extensive tests revealed similar results using evaporated Ni and sputtered indium-tin-oxide (ITO) layers.

Representative I-V measurements and ρ_c extractions for the three contact structures are provided in Figure 1. It can be seen that all contacts exhibit Ohmic I-V behaviour

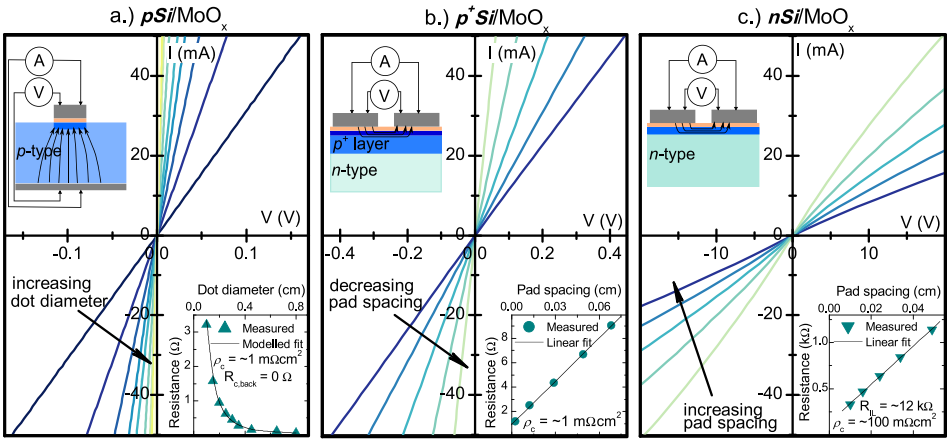

FIG. 1. Current-voltage measurements and ρ_c extractions for (a) ***pSi***/MoO_x, (b) $\boldsymbol{p^+Si}$/MoO_x, and (c) ***nSi***/MoO_x contact structures with a fixed MoO_x interlayer thickness of ~10 nm.

allowing accurate extractions of ρ_c. The correlation of the linear fits to data used in the TLM extraction of ρ_c was high, with R^2 values typically greater than 0.99.

Figure 2(a) presents the measured dependence of ρ_c on MoO_x thickness for the "accumulation" type contacts—***pSi***/MoO_x and ***p*$^+$*Si***/MoO_x. The ρ_c values corresponding to un-annealed, directly metalized ***pSi***/Pd and ***p*$^+$*Si***/Pd contacts are $\rho_c = 10$ mΩ·cm^2 and $\rho_c = 1$ mΩ·cm^2, respectively. Both the ***p*$^+$*Si***/MoO_x and ***pSi***/MoO_x contacts show similar ρ_c trends with MoO_x thickness—an initial decrease in ρ_c relative to the directly metalized surface followed by a gradual increase for thicker MoO_x films—with a local minimum ρ_c of 1 and 0.2 mΩ·cm^2 for ***pSi***/MoO_x and ***p*$^+$*Si***/MoO_x structures with ~10 and 5 nm of MoO_x, respectively. The similarity between the two ρ_c numerical values and trends, despite the use of different contact test structures, support the accuracy of both measurement methods. The minimum ρ_c value for the ***pSi***/MoO_x contact is at the resolution of the measurement technique, shown in Figure 2(a) as a horizontal green line. Therefore, we cannot, with certainty, conclude that ρ_c is lower for the ***p*$^+$*Si***/MoO_x than for the ***pSi***/MoO_x.

A comparison between the ρ_c values measured here and the MoO_x/Pd interface resistivity (measured to be ~0.2 mΩ·cm^2 in other studies[17]) suggests that, particularly in the case of the ***p*$^+$*Si***/MoO_x, the total resistivity may be dominated by the MoO_x/Pd interface.

The initially decreasing ρ_c seen for both "accumulation" contacts could potentially be a result of partial MoO_x surface coverage for the thinner films, as island growth (Volmer-Weber nucleation) is common for thermal evaporation. The increase in ρ_c for MoO_x thickness above 20 nm is likely a consequence of the MoO_x bulk resistivity dominating the total ρ_c. From the measured ρ_c of the thicker structures (30–80 nm of MoO_x), we extract an average dark conductivity σ_{dark} for the MoO_x film of $\sim 2 \times 10^{-5}$ S/cm, which falls towards the lower end of the range reported in the literature, indicating that the film is only slightly sub-stoichiometric. This value is comparable to that of phosphorus or boron doped *a*-Si:H films implemented in silicon heterojunction (SHJ) solar cells.[25]

An analogous plot of the measured J_{0c} dependence on MoO_x thickness for the "accumulation" type contacts is shown in Figure 2(b). It can be seen that both MoO_x coated p-type surfaces produce a J_{0c} of ~200 fA/cm^2 irrespective of (i) the MoO_x thickness; (ii) the surface dopant concentration (***pSi***/$MoO_x \sim 6.8 \times 10^{15}$ cm^{-3} and ***p*$^+$*Si***/$MoO_x \sim 1 \times 10^{19}$ cm^{-3}); and (iii) the application of an overlying Pd layer. The similar J_{0c} values obtained for the two p-type surfaces, despite their vastly different surface dopant concentrations, are consistent with the presence of a strong surface accumulation layer. This point is also supported by the similarities in ρ_c dependence on MoO_x thickness seen for the ***p***MoO_x and ***p*$^+$**MoO_x contacts in Figure 2(a). Regardless of the underlying mechanisms, the almost identical J_{0c} and ρ_c behaviour presented above for the ***pSi***/MoO_x and ***p*$^+$*Si***/MoO_x contacts demonstrates that the MoO_x layer removes the necessity of the boron diffusion.

Figures 3(a) and 3(b) show the measured dependence of ρ_c and the (dark) inversion layer sheet resistance R_{IL} on

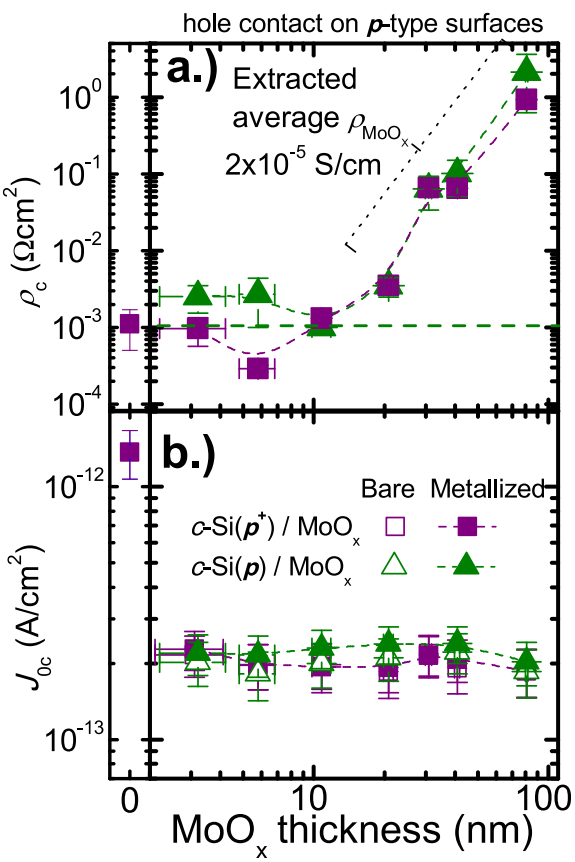

FIG. 2. Dependence of (a) ρ_c and (b) J_{0c} on MoO_x interlayer thickness for the two accumulation type contacts. The straight horizontal line reflects the measurement resolution of the Cox and Strack method for the wafer thickness and resistivity used. Trend lines provide a guide to the eyes only.

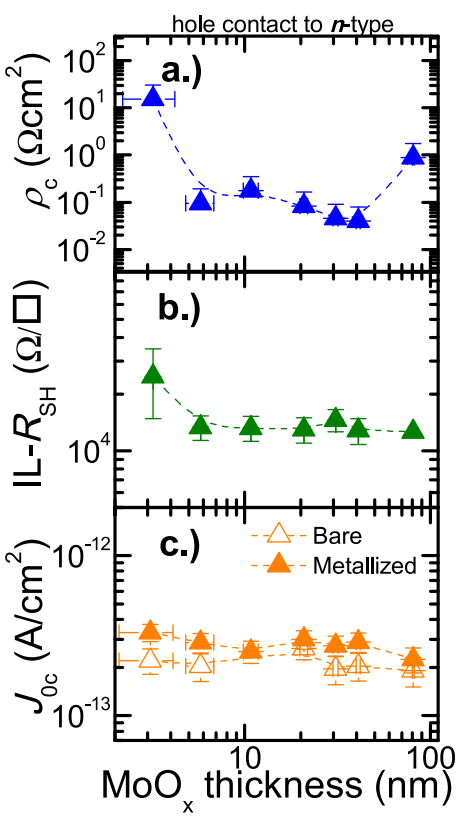

FIG. 3. Dependence of (a) ρ_c, (b) R_{IL}, and (c) J_{0c} on MoO_x interlayer thickness for the ***nSi***/MoO_x inversion type contact. Trend lines provide a guide to the eyes only.

MoO_x thickness for the ***nSi***/MoO_x "inversion" type contact. A ρ_c value for the directly metalized surface could not be measured by the TLM technique due to the absence of a surface inversion layer; however, it is known that making direct metal contact to n-type *c*-Si of moderate resistivity is technologically challenging. Similar to the ρ_c trend in Figure 2(a), an initial decrease in ρ_c with MoO_x thickness is observed, again potentially associated with Volmer-Weber nucleation. After this strong initial reduction, ρ_c decreases slowly from $\sim$150 m$\Omega\cdot$cm^2 to 30 m$\Omega\cdot$cm^2 before increasing in the thickness range of 40–80 nm to a similar ρ_c to that seen for the ***pSi***/MoO_x and ***p$^+$Si***/MoO_x contacts.

As shown in Figure 3(b), the magnitude of R_{IL} initially decreases with MoO_x thickness, consistent with partial surface coverage, before saturating at $\sim$12 k$\Omega/\square$. This sheet resistance is approximately two orders of magnitude higher than the sheet resistance of the n-type Si wafer ($\sim$150 $\Omega/\square$), which confirms that the current flow is confined to the inversion layer by the carrier depletion region formed between it and the n-type substrate, hence supporting the applicability of using the TLM to measure this contact. The $R_{IL} \sim 12\,k\Omega/\square$ measured here is lower than the values reported for inversion layer solar cells, suggesting a higher concentration of holes near the surface.[22,23]

An equivalent inversion layer charge can be calculated from R_{IL} using an average surface hole mobility of 80 cm^2/V, taken from the previous studies on MOSFET devices.[26] From this charge, a corresponding potential at the *c*-Si surface ψ_s can be calculated by assuming Fermi-Dirac statistics. Under these assumptions, ψ_s is calculated to be -0.92 V, with a corresponding hole surface concentration of $\sim 8.6 \times 10^{19}\,cm^{-3}$.

The J_{0c} measurements for the ***nSi***/MoO_x contact as a function of the MoO_x thickness shown in Figure 3(c) follow a similar trend to those in Figure 2(b): J_{0c} is approximately independent of the MoO_x thickness. The non-metalized ***nSi***/MoO_x structures achieve a minimum J_{0c} of $\sim$200 fA/cm^2, which increases to $\sim$300 fA/cm^2 after Pd deposition.

To contextualise these results, it is illustrative to compare them with conventional aluminium and boron p$^+$ hole contacts. The Al alloyed p$^+$, formed by rapid melting and recrystallization of the *c*-Si/Al interface, is typically applied as a rear contact to a p-type wafer and hence is comparable to the ***pSi***/MoO_x contact. The relatively low Al dopant concentration (limited by a solid solubility of $\sim 3 \times 10^{18}\,cm^{-3}$ (Ref. 27)) and the formation of recombination active point defects within the Al doped region generally limit the J_{0c} to between 600 and 900 fA/cm^2,[4,28] although lower values have been reported.[29] Corresponding ρ_c values of 1 to 50 m$\Omega\cdot$cm^2 have been measured for this hole contact.[30,31] The ***pSi***/MoO_x produces lower J_{0c} values for a wide range of MoO_x thicknesses and matches the best reported Al alloyed ρ_c values. The results in this study are especially significant given the moderate doping level of the wafers used for the ***pSi***/MoO_x contacts—suggesting that it may be possible to achieve a low ρ_c on wafers with an even lower doping level, thus mitigating issues such as light-induced bulk lifetime degradation.[32] Improved optical performance, reduced process thermal budget, and the ease by which partial contacts can be applied are all further possible advantages of the ***pSi***/MoO_x contact structure.

The boron p$^+$ contact, typically formed by high temperature (>900 °C) thermal diffusion and subsequent metallization, is the standard hole contact for n-type *c*-Si solar cells and hence can be compared to the ***nSi***/MoO_x contacts presented in this study. Optimised J_{0c} - ρ_c combinations of 400 fA/cm^2 and $\sim$0.1 m$\Omega\cdot$cm^2 can been achieved for metal-contacted heavily doped boron diffused p^{++} contacts.[3,33] In comparison, the optimal J_{0c} obtained for the ***nSi***/MoO_x contact is lower, $J_{0c} \sim 300$ fA/cm^2, but the ρ_c value of $\sim$30 m$\Omega\cdot$cm^2 is considerably higher. Despite that the ***nSi***/MoO_x contact is still adequate for large-area contacts. We have tested such ***nSi***/MoO_x contact via a rudimentary ITO/MoO_x/*c*-Si (n)/*poly*-Si(n$^+$) device with a planar front surface and coarse front contact grid—achieving an open-circuit voltage of $\sim$640 mV measured by the Suns-V_{oc} technique,[34] which is consistent with the J_{0c} value given above. The obtained results for the ***p$^+$Si***/MoO_x also suggest that a partial MoO_x contact could be applied on a light boron diffusion to supersede the selective p^{++} contact approach with improved recombination characteristics and simplified processing.

A remaining challenge is the temperature stability of J_{0c}, which degrades at low temperatures, similar to that found for silicon heterojunction cells. This stability can be improved by the addition of an interlayer, which has also been shown to further improve surface passivation.[10]

In conclusion, thin films of MoO_x deposited by thermal evaporation form excellent hole-selective contacts on both p-type and n-type *c*-Si. The passivation quality of the contacts is independent of the MoO_x thickness, with J_{0c} values of $\sim$200 and $\sim$300 fA/cm^2 for p- and n-type surfaces, respectively. Conversely, ρ_c is found to be strongly dependent on MoO_x thickness. Upper-limit ρ_c values of 1 and 0.2 m$\Omega\cdot$cm^2 have been demonstrated on p and p$^+$ surfaces, respectively. The ρ_c on n-type surfaces is higher, with an optimum value of $\sim$30 m$\Omega\cdot$cm^2, though still applicable to *c*-Si solar cell designs. It is clear that MoO_x films can play a significant role in the development of selective-contacts both in terms of versatility and performance.

The authors wish to thank Lachlan Black and Bénédicte Demaurex for fruitful discussions. This project was partially funded by The Australian Renewable Energy Agency. Equipment at the Australian National Fabrication Facility was utilised for this project.

[1]U. Würfel, A. Cuevas, and P. Würfel, "Charge carrier separation in solar cells," IEEE J. Photovoltaics **PP**(99), 9 (2014).
[2]D. Yan and A. Cuevas, "Empirical determination of the energy band gap narrowing in highly doped n$^+$ silicon," J. Appl. Phys. **114**(4), 044508 (2013).
[3]D. Yan and A. Cuevas, "Empirical determination of the energy band gap narrowing in p$^+$ silicon heavily doped with boron," J. Appl. Phys. **116**, 194505 (2014).
[4]P. Altermatt, S. Steingrube, Y. Yang, C. Sprodowski, T. Dezhdar, S. Koc, B. Veith, S. Herrman, R. Bock, K. Bothe, J. Schmidt, and R. Brendel, "Highly predictive modelling of entire Si solar cells for industrial applications," in Proceedings of the 24th European Photovoltaic Solar Energy Conference (2009).
[5]M. Taguchi, A. Yano, S. Tohoda, K. Matsuyama, Y. Nakamura, T. Nishiwaki, K. Fujita, and E. Maruyama, "24.7% record efficiency HIT solar cell on thin silicon wafer," IEEE J. Photovoltaics **4**(1), 96–99 2014.

[6]K. Masuko, M. Shigematsu, T. Hashiguchi, D. Fujishima, M. Kai, N. Yoshimura, T. Yamaguchi, Y. Ichihashi, T. Mishima, N. Matsubara, T. Yamanishi, T. Takahama, M. Taguchi, E. Maruyama, and S. Okamoto, "Achievement of more than 25%; conversion efficiency with crystalline silicon heterojunction solar cell," IEEE J. Photovoltaics **4**(6), 1433–1435 (2014).
[7]D. Zielke, A. Pazidis, F. Werner, and J. Schmidt, "Organic-silicon heterojunction solar cells on n-type silicon wafers: The BackPEDOT concept," Sol. Energy Mater. Sol. Cells **131**, 110–116 (2014).
[8]J. Schmidt, V. Titova, and D. Zielke, "Organic-silicon heterojunction solar cells: Open-circuit voltage potential and stability," Appl. Phys. Lett. **103**(18), 183901 (2013).
[9]C. Battaglia, X. Yin, M. Zheng, I. D. Sharp, T. Chen, S. McDonnell, A. Azcatl, C. Carraro, B. Ma, R. Maboudian, R. M. Wallace, and A. Javey, "Hole selective MoO_x contact for silicon solar cells," Nano Lett. **14**(2), 967–971 (2014).
[10]C. Battaglia, S. M. de Nicolas, S. De Wolf, X. Yin, M. Zheng, C. Ballif, and A. Javey, "Silicon heterojunction solar cell with passivated hole selective MoO_x contact," Appl. Phys. Lett. **104**(11), 113902 (2014).
[11]S. Avasthi, W. E. McClain, G. Man, A. Kahn, J. Schwartz, and J. C. Sturm, "Hole-blocking titanium-oxide/silicon heterojunction and its application to photovoltaics," Appl. Phys. Lett. **102**(20), 203901 (2013).
[12]J. Jhaveri, S. Avasthi, K. Nagamatsu, and J. Sturm, "Stable low-recombination n-Si/TiO2 hole-blocking interface and its effect on silicon heterojunction photovoltaics," in IEEE 40th Photovoltaic Specialist Conference (PVSC) (2014).
[13]G. G. Untila, T. N. Kost, A. B. Chebotareva, M. B. Zaks, A. M. Sitnikov, O. I. Solodukha, and M. Z. Shvarts, "Bifacial low concentrator argentum free crystalline silicon solar cells based on ARC of TCO and current collecting grid of copper wire," AIP Conf. Proc. **1556**(1), 106 (2013).
[14]G. Untila, T. Kost, A. Chebotareva, and M. Timofeyev, "Optimization of the deposition and annealing conditions of fluorine-doped indium oxide films for silicon solar cells," Semiconductors **47**(3), 415–421 (2013).
[15]J. Meyer, S. Hamwi, M. Kroger, W. Kowalsky, T. Riedl, and A. Kahn, "Transition metal oxides for organic electronics: Energetics, device physics and applications," Adv. Mater. **24**(40), 5408–5427 (2012).
[16]S. McDonnell, A. Azcatl, R. Addou, C. Gong, C. Battaglia, S. Chuang, K. Cho, A. Javey, and R. M. Wallace, "Hole contacts on transition metal dichalcogenides: Interface chemistry and band alignments," ACS Nano **8**(6), 6265–6272 (2014).
[17]S. Chuang, C. Battaglia, A. Azcatl, S. McDonnell, J. S. Kang, X. Yin, M. Tosun, R. Kapadia, H. Fang, R. M. Wallace, and A. Javey, "MoS_2 p-type transistors and diodes enabled by high work function MoOx contacts," Nano Lett. **14**(3), 1337–1342 (2014).
[18]M. T. Greiner, L. Chai, M. G. Helander, W.-M. Tang, and Z.-H. Lu, "Transition metal oxide work functions: The influence of cation oxidation state and oxygen vacancies," Adv. Funct. Mater. **22**(21), 4557–4568 (2012).
[19]R. Swanson and D. Kane, "Measurement of the emitter saturation current by a contactless photoconductivity decay method," in Proceedings of 18th IEEE Photovoltaic Specialists Conference (1985).
[20]K. R. McIntosh and L. E. Black, "On effective surface recombination parameters," J. Appl. Phys. **116**(1), 014503 (2014).
[21]S. S. Cohen, "Contact resistance and methods for its determination," Thin Solid Films **104**(3), 361–379 (1983).
[22]M. Grauvogl and R. Hezel, "The truncated-pyramid MIS inversion-layer solar cell: A comprehensive analysis," Prog. Photovoltaics **6**(1), 15–24 (1998).
[23]F. Werner, Y. Larionova, D. Zielke, T. Ohrdes, and J. Schmidt, "Aluminum-oxide-based inversion layer solar cells on n-type crystalline silicon: Fundamental properties and efficiency potential," J. Appl. Phys. **115**(7), 073702 (2014).
[24]R. Cox and H. Strack, "Ohmic contacts for GaAs devices," Solid-State Electron. **10**(12), 1213–1218 (1967).
[25]M. Tucci, L. Serenelli, S. De Iuliis, M. Izzi, G. de Cesare, and D. Caputo, *Contact Formation on a-Si:H/c-Si Heterostructure Solar Cells in Physics and Technology of Amorphous-Crystalline Heterostructure Silicon Solar Cells*, edited by W. G. J. H. M. van Sark, L. Korte, and F. Roca (Springer, 2011), pp. 331–376.
[26]S. Sze and K. Ng, *Physics of Semiconductor Devices* (John Wiley & Sons, 2006).
[27]P. Lolgen, W. Sinke, C. Leguijt, A. Weeber, P. Alkemade, and L. Verhoef, "Boron doping of silicon using coalloying with aluminium," Appl. Phys. Lett. **65**(22), 2792–2794 (1994).
[28]J. Muller, K. Bothe, S. Gatz, H. Plagwitz, G. Schubert, and R. Brendel, "Contact formation and recombination at screen-printed local aluminum-alloyed silicon solar cell base contacts," IEEE Trans. Electron Devices **58**(10), 3239–3245 (2011).
[29]R. Woehl, P. Gundel, J. Krause, K. Ruhle, F. Heinz, M. Rauer, C. Schmiga, M. Schubert, W. Warta, and D. Biro, "Evaluating the aluminum-alloyed p^+-layer of silicon solar cells by emitter saturation current density and optical microspectroscopy measurements," IEEE Trans. Electron Devices **58**(2), 441–447 (2011).
[30]A. Rohatgi, S. Narasimha, and D. S. Ruby, "Effective passivation of the low resistivity silicon surface by a rapid thermal oxide/PECVD silicon nitride stack and its application to passivated rear and bifacial Si solar cells," in Proceedings of the 2nd World Conference on Photovoltaic Solar Energy Conversion (1998).
[31]E. Urrejola, K. Peter, H. Plagwitz, and G. Schubert, "Al-Si alloy formation in narrow p-type Si contact areas for rear passivated solar cells," J. Appl. Phys. **107**(12), 124516 (2010).
[32]J. Schmidt and K. Bothe, "Structure and transformation of the metastable boron- and oxygen-related defect center in crystalline silicon," Phys. Rev. B **69**, 024107 (2004).
[33]C. Mader, J. Muller, S. Eidelloth, and R. Brendel, "Local rear contacts to silicon solar cells by in-line high-rate evaporation of aluminum," Sol. Energy Mater. Sol. Cells **107**, 272–282 (2012).
[34]R. Sinton and A. Cuevas, "A quasi-steady-state open-circuit voltage method for solar cell characterization," in *16th European Photovoltaic Solar Energy Conference* (2000), Vol. 25.